Kelly L. Keeling, Okki Cho, Denis B. Scanlon, Grant W. Booker, Andrew D. Abell and Kate L. Wegener

The key position: influence of staple location on constrained peptide conformation and binding

Organic & Biomolecular Chemistry, 2016; 14(41):9731-9735

Published at: http://dx.doi.org/10.1039/c6ob01745b

Journal Name

ARTICLE

The Key Position: Influence of Staple Location on Constrained Peptide Conformation and Binding

Received 00th January 20xx,
Accepted 00th January 20xx

DOI: 10.1039/x0xx00000x

www.rsc.org/

Kelly L. Keeling,[a] Okki Cho,[b] Denis B. Scanlon,[a] Grant W. Booker,[b] Andrew D. Abell[c] and Kate L. Wegener*[b]

Constrained α-helical peptides are showing potential as biological probes and therapeutic agents that target protein-protein interactions. However, the factors that determine the optimal constraint locations are still largely unknown. Using the β-integrin/talin protein interaction as a model system, we examine the effect of constraint location on helical conformation, as well as binding affinity, using circular dichroism and NMR spectroscopy. Stapling increased the overall helical content of each integrin-based peptide tested. However, NMR analysis revealed that different regions within the peptide are stabilised, depending on constraint location, and that these differences correlate with the changes observed in talin binding mode and affinity. In addition, we show that examination of the atomic structure of the parent peptide provides insight into the appropriate placement of helical constraints.

Introduction

Molecules that mimic the binding topography of a protein-protein interaction (PPI) provide an attractive and expedient route to potential therapeutics for the treatment of important diseases[1, 2]. Peptide fragments derived from the binding interface of a PPI are an important starting point for the rational design of such ligands. However, these fragments usually lack conformational stability, and as such are often modified to promote the structure attained in the native protein. α-Helical 'stapled' peptides are a prime example of this, where helical conformation is stabilized by a side-chain to side-chain covalent linker[3, 4]. The restriction in conformational freedom reduces the entropic cost of binding. However, not all constraint locations produce peptides with improved affinity, despite increased α-helicity[5]. While linker location is dictated by factors such as avoiding steric interference with the binding interface and optimizing the nucleation of helicity, screening many linker positions is generally required to find the optimum analogue[6]. A better understanding of the effects of linker locations on conformation and hence binding affinity, would lead to improved strategies for peptide design.

Here we investigate, and begin to define, the relationship between conformation, biological affinity and tether location, using constrained peptides derived from the β3-integrin/talin PPI. This interaction is critical for integrin activation, and triggers platelet aggregation and thrombosis formation[7]. Disruption of this PPI therefore offers a novel approach to anti-platelet therapeutics for the treatment of heart disease[8, 9]. Integrin binding to talin occurs over an extensive surface, comprised of two main regions, termed the membrane proximal (MP) and membrane distal (MD) interfaces[10], with an overall Kd in the range of 270-600μM[11, 12]. The MP integrin region, which binds as an α-helix (Figure 1a), is crucial for integrin activation[10]. Here we report a series of lactam-bridged analogues of the helical region of the β3 integrin cytoplasmic tail, in which we vary the location of the lactam staple. Detailed structural characterisation of the peptides allowed us to rationalise the influence of linker location on structure and affinity.

Results and discussion

Design and synthesis of stapled peptides

'Hot spot' residues within the β3-integrin membrane proximal region (Figure 1D) were identified using the Robetta online alanine scan server[13] (Table S1). Three of the four key residues identified by this scan (F727, F730, and W739) are known to be important for both talin binding and integrin activation[10, 11, 14] while the fourth, E733 has been shown to influence integrin activation[15]. Evidence of salt bridge formation between integrin D723 and talin residue K327 in the crystal structure of the related integrin β1D bound to talin F2-F3[16], resulted in D723 also being classed as a hotspot residue. Linker positions were chosen so as not to interfere with these sites, resulting in constraints at positions A, B and C (Figure 1, Table 1). Modelling of these staple locations, using the talin/integrin complex structure 2H7E, also predicted that these linkers were unlikely to interfere with the interaction. Linkage at position D was also included, for comparison.

[a] Department of Chemistry, School of Physical Sciences, The University of Adelaide, Adelaide, South Australia, 5005.
[b] Department of Molecular and Cellular Biology, School of Biological Sciences, The University of Adelaide, Adelaide, South Australia 5005. Email: kate.wegener@adelaide.edu.au
[c] Department of Chemistry and Centre for Nanoscale BioPhotonics, The University of Adelaide, Adelaide, South Australia, 5005.
† Electronic Supplementary Information (ESI) available. See
DOI: 10.1039/x0xx00000x

The linear peptide (βMP) and linear precursors of βLAC-A to D were synthesized by Fmoc solid-phase peptide synthesis protocols17. Constraints were incorporated by lactamization of lysine and aspartic acid residues introduced in the i and i+4 positions, respectively18, 19 (Table 1) (See † ESI for detail).

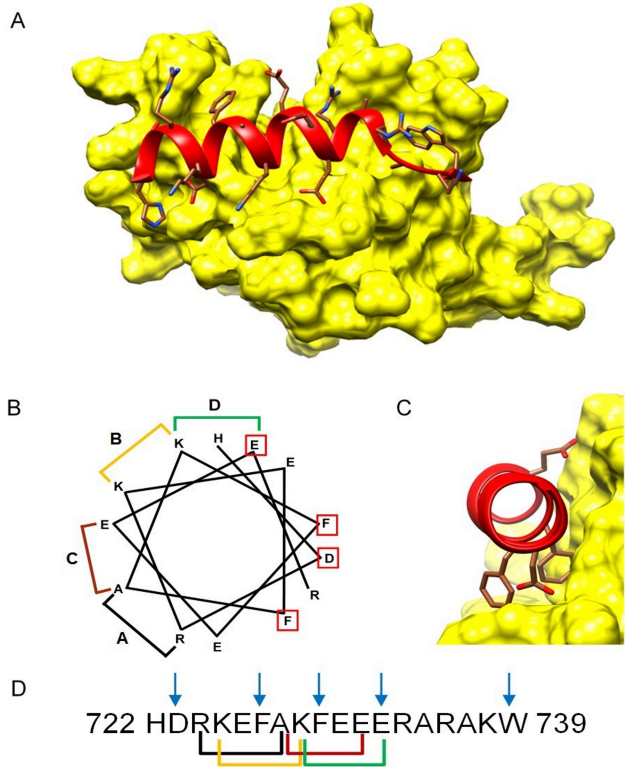

Figure 1. (A) Structure of talin bound to the MP region of the β3 integrin tail (derived from PDB: 2H7D). (B) Wheel diagram of the MP helix. (C) Integrin hot spot side-chains contacting talin F3 (D) βMP peptide sequence. (B) and (D) indicate hot-spot residues (boxes/arrows) and linker locations: A (black), B (yellow), C (red), and D (green).

Helical content of stapled peptides

All lactam-constrained peptides were predicted to have increased helicity in comparison with the unconstrained parent peptide β3MP. To verify this, CD spectra were acquired for the lactam bridged peptides βLAC-A to D. The spectra obtained show characteristic spectral features associated with α-helical structure, indicated by minima at 208 and 222nm. All constrained peptides demonstrated helical stabilization, with increases in overall helical content of between 19-34%, compared to the linear peptide βMP (Table 1 and Figure S1).

Table 1. Sequences, helicity, and affinity of β3 integrin-derived peptides.

Compound	Sequence	Helicity[a]	Kd (mM)[b]
βMP	HDRKEFAKFEEERARAKW	23%	5.4 ± 0.2
βLAC-A	HD**K***KEF**D***KFEEERARAKW	48%	2.7 ± 0.1
βLAC-B	HDR**K***EFA**D***FEEERARAKW	57%	0.94 ± 0.02
βLAC-C	HDRKEF**K***KFE**D***ERARAKW	42%	7.0 ± 0.3
βLAC-D	HDRKEFA**K***FEE**D***RARAKW	51%	6.5 ± 0.3

[a] Calculated from mean residue molar ellipticity at 222nm, using 25μM peptide in 10mM phosphate (pH 6.1) at 298K (see ESI for details). [b] Kd values are given ± fitting error

Talin binding affinity of stapled peptides

The effect of constraint position on peptide affinity for the talin F3 domain was determined by recording ^{15}N-HSQC spectra of ^{15}N-labelled talin, with increasing concentrations of unlabelled peptides. Somewhat surprisingly, only βLAC-A and βLAC-B demonstrated enhanced binding affinity compared to βMP (Table 1, Figure S2). The greatest enhancement was seen for βLAC-B, which resulted in a more than 5-fold increase in binding affinity for talin, making it comparable to the full-length integrin tail[11, 12]. Lactam constraint at positions C and D resulted in modest decreases in affinity. For βLAC-D, this could be explained by modification of the hotspot residue E(733). However, the decreased affinity of βLAC-C was unexpected, prompting further analysis to determine the basis of the effect of bridge location on talin binding affinity.

Three dimensional peptide structures

To understand the difference in binding of the peptide series, ^{1}H homonuclear NMR spectroscopy was used to probe the 3D solution structures of βLAC-A to D. Peptide resonances were assigned, and a range of secondary structure indicators determined, as summarized in Figure S3. Structures were also generated, using NOE, scalar coupling and hydrogen bond restraints, and the ARIA program[20] (Figure 2).

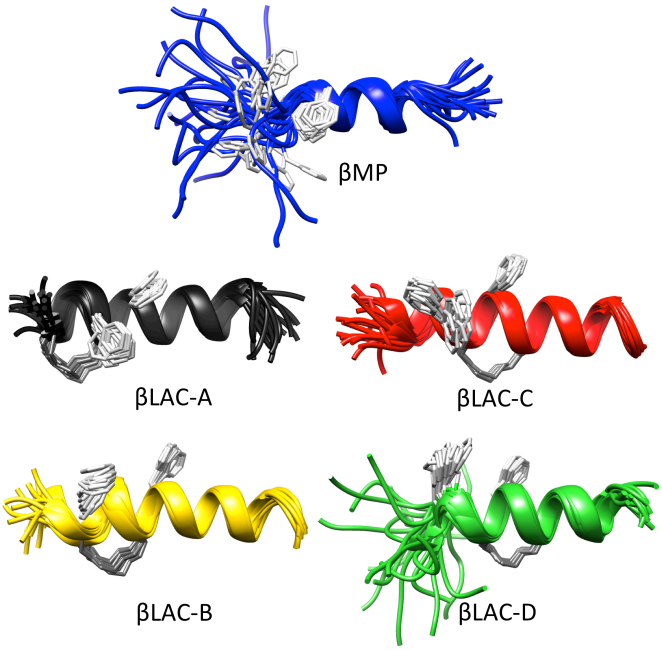

Figure 2. NMR structures for βMP and βLAC-A to D, superimposed over the backbone atoms of the well-defined residues. Structures were determined for peptides (~5mM) in 50mM phosphate buffer (pH 6.1), with 100mM NaCl, at 298K. The key binding residues F727 and F730, and the lactam constraints, are indicated in light and dark grey, respectively.

We first examined the unconstrained parent peptide, βMP. This peptide had upfield shifted αH chemical shifts, and downfield shifted NH resonances, relative to random coil values for residues 730 to 736 (Figure S4), indicating helical structure in the C-

terminus only[21, 22]. Supporting this, four of the five measurable $^3J_{HNH\alpha}$ couplings from the C-terminal region were less than 6Hz, consistent with helical φ angles[23]. In addition, βMP had seven residues with amide proton (NH) temperature coefficients greater than -4 ppb/K, indicative of their involvement in hydrogen-bonds, and these NHs were all found in the C-terminus of the peptide. αβ(i,i+3) and αN(i,i+3) NOE connectivities also support helical structure in this region of the peptide (Figure S5), and the ARIA structures generated were consistent with this (Figure 2).

Interestingly, analysis of the relative αN and NN NOE intensities for βMP suggests extended or random coil structure, present along the length of the peptide. This apparent contradiction is likely due to the peptide being only weakly structured in solution (23% by CD), with the peptide moving between extended and helical conformations. The NMR structures are dominated by the helical form of the peptide, because of the need to satisfy the mid-range NOEs that are observed for helices. Nevertheless, the structures suggest that the helical content of the peptide is mainly present in the C-terminal half of the peptide.

NMR data for each of the lactam constrained peptides show evidence of increased helical structure when compared to the parent peptide (Figure S3). However, the extent of helicity differs between peptides, with the helical region beginning in each case around the location of the constraint and extending to the C-terminus, indicating helicity is nucleated in this direction. In contrast to βMP, NOE intensity ratios for the constrained peptides support helical structure, suggesting more stable structures, consistent with the CD data. αH resonances are largely upfield shifted, apart from a break at the linker aspartate, likely due to shorter hydrogen bonds between the lactam residue backbone atoms‡. Structures were calculated for each constrained peptide (Figure 2, Table S2) using a version of ARIA modified to handle lactam side-chain/side-chain constraints (Benjamin Bardiaux, Unite de Bioinformatique Structurale, Institut Pasteur). The regions of helicity identified in these structures are similar to those inferred from the raw NMR data (Figure S3, Table S3).

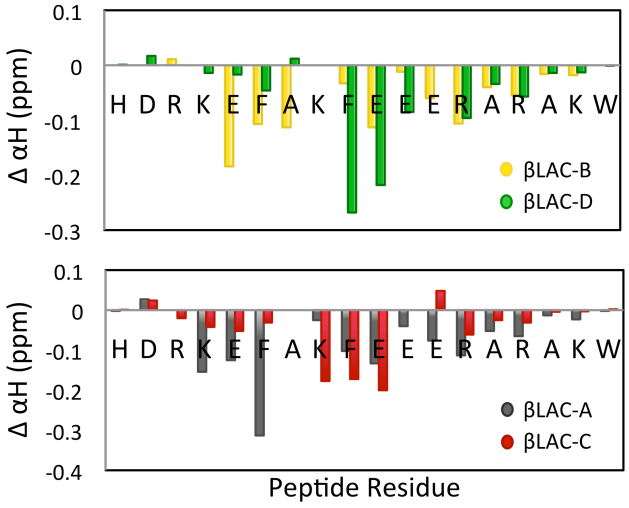

Figure 3. Difference in αH shifts between the lactam constrained peptides, and the parent βMP peptide (linker residues not shown). B (yellow), D (green), A (black), and C (red).

Helicity is initiated in each peptide at the location of the linker. Thus, βLAC-A and B are essentially helical along the peptide's length, while βLAC-C and D have more disordered *N*-terminal regions, similar to the parent peptide. This can clearly be seen from a plot of the difference in αH chemical shift between the linear and constrained peptides (Figure 3). The negative differences, observed for almost all residues, indicate the constrained peptides have greater helicity than the original peptide. However, the greatest changes for βLAC-A and B are observed in the *N*-terminal region, with smaller changes for residues in the remainder of the sequence. This indicates greatly increased helical content of the N-terminus, and stabilization of the already helical *C*-terminal region. Conversely, lactams βLAC-C and D appear to stabilize helical structure in the vicinity of the linker, with relatively minor increases in helicity outside of this region.

Resistance of stapled peptides toward proteolytic cleavage

To further investigate structural propensity around the linker site, we took advantage of predicted chymotrypsin cleavage sites at F727 and F730. Chymotrypsin-treated βMP degraded rapidly, with a half-life of 14 minutes, and cleavage only observed following F727 (Figure S6). In contrast, more than 95% of βLAC-B remained after treatment with chymotrypsin for 90 minutes, after which protease activity began to decline. βLAC-D was similarly treated, and at 90 minutes more than 50% of this peptide remained intact. These results are consistent with the greater helical structure induced here by constraint at position B, over position D.

Analysis of the binding mode of stapled integrin peptides

To assess the likelihood of the lactam staples directly interacting or hindering the talin-binding interface, the calculated peptide structures were superimposed onto the talin/β3-integrin structure (PDB 2H7E, Figure S7). Lactams A-C were clearly distant from the interfacial region, while a small number of clashes occurred for lactam D, as well as disruption of the hydrogen bond between peptide residue 733 and S362 from talin. The lack of affinity improvement for βLAC-D could be explained by these disruptions. However, the interaction between βLAC-C and talin is not likely to be influenced by steric hindrance of the staple.

Remarkably, the structural differences observed between the lactam A/B and C/D pairs, correlated with differences in how the peptides interact with talin, as revealed by the pattern of talin residues perturbed by each peptide in the NMR titrations (Figure 4). Previously, it has been shown that full engagement of the integrin MP helix perturbs a distinct subset of talin resonances[10], designated here as region H. However, integrin fragment βMP perturbed region H only weakly, with the greatest effects observed instead in regions associated with binding of the C-terminal tryptophan (region W). The same pattern was also observed for the poorly binding βLAC-C and D peptides. In contrast, βLAC-A and B had markedly increased influence on region H of talin, suggesting that constraint in these positions, allowed correct engagement of the full peptide helix.

βLAC-A and B each had increased helical content for the hot-spot residue F727 (cf. βLAC-C and D). Thus, the relative positions of key side chains F727 and F730 are better defined, which is reflected in improved binding affinity. Precisely why the

improvement is greater for βLAC-B rather than A is not known, but is likely due to subtle differences in conformation and dynamics. Our data suggest that for βLAC-A there is some disruption of helicity at residue K729, located between the two key phenylalanines ($I_{\alpha N}/I_{NN}$ and $I_{\alpha N}/I_{\alpha N}$ >1, and random coil-like αH chemical shifts (Figure S3)). However, further investigation would be necessary to verify this is the cause of the reduced affinity.

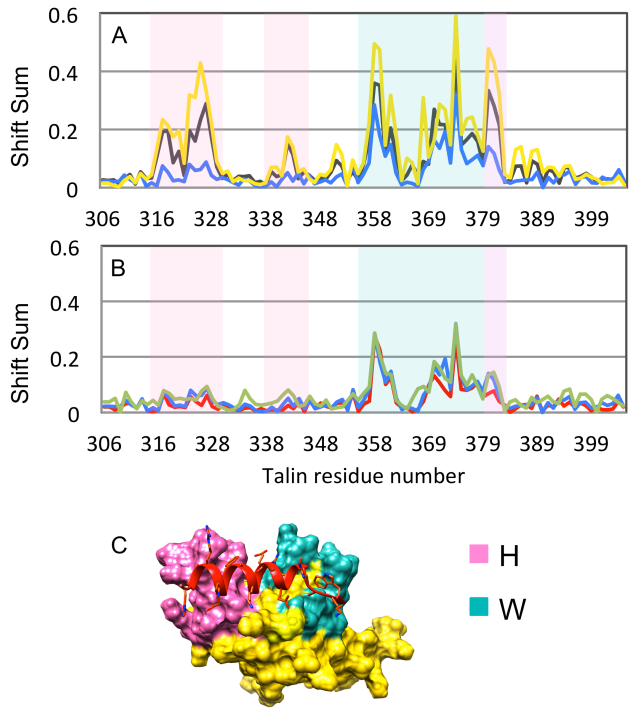

Figure 4. Combined secondary shifts of amide ^{15}N and ^{1}H resonances induced by peptide addition to talin. (A) βLAC-A (-) and B (-), or (B) βLAC-C (-) and D (-), are compared to shifts induced by βMP (-). Regions affected by engagement of the β-integrin helix (H) are highlighted in pink, and those affected by W739 in teal. The surface representation of these regions is shown in (C).

Conclusions

Two important points emerged from our study on the effect of staple location on peptide conformation and affinity: 1) staples were found to differentially influence local helical structure, depending on location, and 2) knowledge of parent peptide structure can identify regions that most require stabilisation.

We found that, while all lactam staples increased the overall helical content of integrin peptides, NMR analysis indicated differences in the specific residues stabilised for each location variant. Helical stabilisation was greatest around the staple itself, with some additional stabilisation occurring to the peptide region C-terminal of the constraint. Helicity was not found to nucleate to the N-terminal side of the staple. Importantly, these differences in local structure had a direct impact on both talin binding mode and affinity: only stabilisation of the unstructured N-terminus, allowed full peptide engagement with talin. This leads on to the second point: that a detailed understanding of parent peptide structure can identify optimal regions for constraint, by revealing poorly structured regions near key binding residues. Such a strategy, when combined with knowledge of the binding interface, can be applied when limited resources prevent thorough screening of alternate linker locations. Overall, this study revealed the importance of detailed structural analysis of peptides for greater understanding of the role and impact of covalent constraints.

This work is also a first step in the development of peptide-based inhibitors of the talin-integrin protein-protein interaction. We have identified peptides that selectively target talin's integrin binding site, with similar affinity to that of full-length β3-integrin tail. It may be possible to enhance affinity further still, through incorporation of multiple or longer (i,i+7) staples, and/or siting linkers such that the linker itself contributes to the binding interface[24-26]. In future work, we will explore these possibilities, as well as examine the cellular uptake and biological action of these peptides. The stapled integrin-based peptides generated here provide important leads to a new class of anti-thrombotic therapeutic with a novel mechanism of action.

Acknowledgements

ARC Discovery Grant (DP120100582) funded this work. K.W. is supported by a Ramsay Fellowship, the University of Adelaide. We thank ANFF for equipment funding and Benjamin Bardiaux, Unite de Bioinformatique Structurale, Institut Pasteur, for providing a modified ARIA program, for lactam peptide structural calculations.

Notes and references

‡ NMR data for the stapled peptides revealed that while the calculated structures had unbroken helicity from the linker to the C-terminus, helical αH and NH secondary shifts were inevitably interrupted at the aspartate linker residue (i+4) (Figure S4). NMR analysis also revealed the aspartate linker residues had unusually large and negative NH temperature coefficients, despite being consistently hydrogen bonded in the calculated structures. Previous reports suggest that both NH temperature coefficients and NH secondary shifts are influenced by hydrogen bond length[22, 27]. Shorter hydrogen bonds (< 2 Å) are associated with downfield shifted NH resonances and temperature coefficients less than -4ppb/K, while bonds longer than 2Å are shifted upfield and have temperature coefficients greater than -4ppb/K. Scrutiny of the calculated lactam structures confirms all calculated aspartate linker NH hydrogen bonds were less than 2Å, however other hydrogen bonds were also found to have distances in this range (data not shown). It is possible that the presence of the lactam amide functional group might be influencing residue i+4 secondary shifts and temperature coefficients, however the downfield shifted NH suggests a deshielding effect of the lactam, while the unusually large and negative NH temperature coefficient is more consistent with a shielding effect from this group[27]. Similar effects on linker αH and temperature coefficients were found for constrained peptides studied by Hoang et al.[28]. These were attributed to local distortion of the helical structure, however no such distortion was evident in the NMR structures calculated for our integrin-derived peptides. Thus, we believe the hydrogen bond length explanation to be more plausible.

Structures, chemical shifts and restraints used in calculations, have been deposited in the Biological Magnetic Resonance Data Bank (BMRB): B3MP: 21074, BLACA: 21075, BLACB: 21076, BLACC: 21077, BLACD: 21078.

1. V. Azzarito, K. Long, N. S. Murphy and A. J. Wilson, *Nat. Chem.*, 2013, **5**, 161-173.
2. M. Pelay-Gimeno, A. Glas, O. Koch and T. N. Grossmann, *Angew. Chem. Int. Ed. Engl.*, 2015, **54**, 8896-8927.
3. G. L. Verdine and G. J. Hilinski, in *Method. Enzymol.*, eds. K. D. Wittrup and L. V. Gregory, Academic Press, 2012, vol. 503, pp. 3-33.
4. Y. H. Lau, P. de Andrade, Y. Wu and D. R. Spring, *Chem. Soc. Rev.*, 2015, **44**, 91-102.
5. T. Okamoto, K. Zobel, A. Fedorova, C. Quan, H. Yang, W. J. Fairbrother, D. C. S. Huang, B. J. Smith, K. Deshayes and P. E. Czabotar, *ACS Chem. Biol.*, 2012, **8**, 297-302.
6. L. D. Walensky and G. H. Bird, *J Med Chem*, 2014, **57**, 6275-6288.
7. B. G. Petrich, P. Marchese, Z. M. Ruggeri, S. Spiess, R. A. Weichert, F. Ye, R. Tiedt, R. C. Skoda, S. J. Monkley, D. R. Critchley and M. H. Ginsberg, *J Exp Med*, 2007, **204**, 3103-3111.
8. B. G. Petrich, P. Fogelstrand, A. W. Partridge, N. Yousefi, A. J. Ablooglu, S. J. Shattil and M. H. Ginsberg, *J. Clin. Invest.*, 2007, **117**, 2250-2259.
9. B. Shen, X. Zhao, K. A. O/'Brien, A. Stojanovic-Terpo, M. K. Delaney, K. Kim, J. Cho, S. C. T. Lam and X. Du, *Nature*, 2013, **503**, 131-135.
10. K. L. Wegener, A. W. Partridge, J. Han, A. R. Pickford, R. C. Liddington, M. H. Ginsberg and I. D. Campbell, *Cell*, 2007, **128**, 171-182.
11. N. J. Anthis, K. L. Wegener, D. R. Critchley and I. D. Campbell, *Structure*, 2010, **18**, 1654-1666.
12. D. T. Moore, P. Nygren, H. Jo, K. Boesze-Battaglia, J. S. Bennett and W. F. DeGrado, *PNAS*, 2012, **109**, 793-798.
13. T. Kortemme, D. E. Kim and D. Baker, *Sci. STKE*, 2004, **2004**, p12.
14. S. Tadokoro, S. J. Shattil, K. Eto, V. Tai, R. C. Liddington, J. M. de Pereda, M. H. Ginsberg and D. A. Calderwood, *Science*, 2003, **302**, 103-106.
15. F. Saltel, E. Mortier, V. P. Hytönen, M.-C. Jacquier, P. Zimmermann, V. Vogel, W. Liu and B. Wehrle-Haller, *J. Cell Biol.*, 2009, **187**, 715-731.
16. N. J. Anthis, K. L. Wegener, F. Ye, C. Kim, B. T. Goult, E. D. Lowe, I. Vakonakis, N. Bate, D. R. Critchley, M. H. Ginsberg and I. D. Campbell, *EMBO J.*, 2009, **28**, 3623–3632.
17. R. Sheppard, *J. Pept. Sci.*, 2003, **9**, 545-552.
18. A. D. de Araujo, H. N. Hoang, W. M. Kok, F. Diness, P. Gupta, T. A. Hill, R. W. Driver, D. A. Price, S. Liras and D. P. Fairlie, *Angew. Chem. Int. Ed.*, 2014, **53**, 6965-6969.
19. N. E. Shepherd, H. N. Hoang, G. Abbenante and D. P. Fairlie, *JACS*, 2005, **127**, 2974-2983.
20. W. Rieping, M. Habeck, B. Bardiaux, A. Bernard, T. E. Malliavin and M. Nilges, *Bioinformatics*, 2007, **23**, 381-382.
21. D. S. Wishart, B. D. Sykes and F. M. Richards, *Biochemistry*, 1992, **31**, 1647-1651.
22. G. Wagner, A. Pardi and K. Wuethrich, *JACS*, 1983, **105**, 5948-5949.
23. A. Pardi, M. Billeter and K. Wüthrich, *J. Mol. Biol.*, 1984, **180**, 741-751.
24. M. L. Stewart, E. Fire, A. E. Keating and L. D. Walensky, *Nat Chem Biol*, 2010, **6**, 595-601.
25. S. Baek, P. S. Kutchukian, G. L. Verdine, R. Huber, T. A. Holak, K. W. Lee and G. M. Popowicz, *JACS*, 2012, **134**, 103-106.
26. C. Phillips, L. R. Roberts, M. Schade, R. Bazin, A. Bent, N. L. Davies, R. Moore, A. D. Pannifer, A. R. Pickford, S. H. Prior, C. M. Read, A. Scott, D. G. Brown, B. Xu and S. L. Irving, *JACS*, 2011, **133**, 9696-9699.
27. T. Cierpicki and J. Otlewski, *J. Biomol. NMR*, 2001, **21**, 249-261.
28. H. N. Hoang, R. W. Driver, R. L. Beyer, T. A. Hill, A. D. de Araujo, F. Plisson, R. S. Harrison, L. Goedecke, N. E. Shepherd and D. P. Fairlie.